APPROCHER LES DEUX INFINIS PAR LES ONDES ELECTROMAGNETIQUES

Interféromètre de mesure de phase atmosphérique pour l'observatoire NOEMA

Atmospheric Phase Monitoring Interferometer for the NOEMA Observatory

S. Mahieu[1], B. Pissard[1], M. Bremer[1], C. Risacher[1], R. Blundell[2], R. Kimberk[2], J. Test[2]

[1] Institut de Radio Astronomie Millimétrique, IRAM, 300 rue de la piscine, 38400 Saint Martin d'Hères, France.
[2] Harvard-Smithsonian Center for Astrophysics, 60 Garden Street, Cambridge, MA 02138, USA.

Interféromètre, phase atmosphérique, NOEMA.
Interferometer, Atmospheric phase, NOEMA.

Résumé/Abstract

L'IRAM adapte, en collaboration avec le Smithsonian Astrophysical Observatory (SAO), un système de contrôle de la phase atmosphérique, comme développé pour l'observatoire submillimétrique SMA, qui sera potentiellement utilisé à l'observatoire NOEMA (NOrthern Extended Millimeter Array).

IRAM is currently adapting, in collaboration with the Smithsonian Astrophysical Observatory (SAO), an atmospheric phase monitoring system as was developed for the Submillimeter Array (SMA) to be possibly used for the NOEMA (NOrthern Extended Millimeter Array) interferometer.

1 Introduction

In this paper, we present the proof-of-concept of an atmospheric phase monitoring system and show the first results obtained so far.

Millimeter wave astronomical interferometers combine signals received from cosmic radio sources that reach multiple antennas (soon twelve 15 meters antennas for the NOEMA case) to produce maps of the sky. Direction of the source and geometry of the array of antennas allows the signals to be combined with a predictable phase. Trouble is that signal propagation can be altered by atmospheric turbulences. Indeed, in the troposphere, water vapor plays a particularly important role in radio signals propagation, its refractivity being about 20 times greater in the radio range than in the near-infrared or optical regimes. The phase fluctuations in radio interferometers at millimeter and centimeter wavelengths are predominantly caused by fluctuations in the distribution of water vapor. Therefore, implementing such a phase monitor interferometer would provide us with a permanent monitoring system of the observing conditions for the NOEMA interferometer, located on the plateau de Bure, at 2550m above sea level in the French Alps. This system would make observations more efficient, by being able to choose the correct observing band right away and/or anticipate on whether to start or stop observing.

2 System description.

The atmospheric phase monitoring system demonstrator is based on a dual off- axis aluminium satellite dishes (Fuba DDA 110: 1090 x 991 mm^2) interferometer, that receive a broadband white noise-like Ku Band signal from a geostationary satellite and focus it to the center of the feed signal source. (see Figure 1)

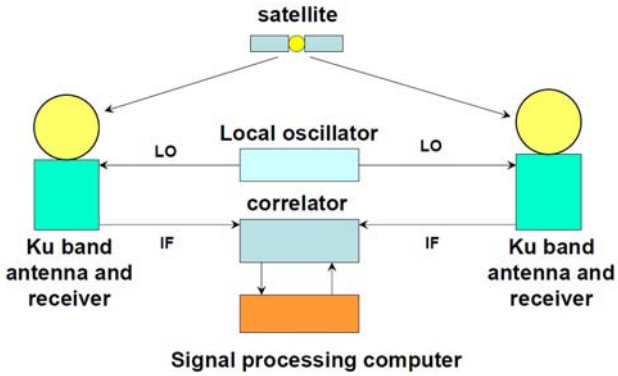

Figure 1: Phase Monitoring System Principle

The Low Noise Blocks (LNB) that down convert this signal to the Intermediate Frequency (IF) one (~1.2 GHz) are commercial satellite system receivers that have been modified to be fed with a common Local Oscillator (LO) signal through a SMA connector that integrates a spring loaded contact, once the original Dielectric Resonator Oscillator (DRO) is removed (see Figure 2).

Figure 2: Technomate Low Noise Block downconverter. Left: LO injection on the body, middle: LO circuit with Dielectric Resonator Oscillator, Right: SMA connector that integrates a spring loaded contact for LO signal injection.

The IF signals are then amplified, filtered and transported through optical fibres down to the rack that is located in the building where they are processed by a commercial analog correlator (IQ demodulation card) that produces the phase delays between pairs (only one so far) of antennas from the I & Q signals.

The data are then sampled at 10Hz and further processed by a LINUX pc that runs software which tracks the Walsh cycle and applies sign changes to remove offsets in Q and I signals. It determines the phase angle from arctan Q/I and calculates a least squares sine fit to the unwrapped phase, subtracts that from the unwrapped phase and then calculates the rms values from the residuals.

The Figure 3 below shows the schematic of the overall phase monitoring system, with two antennas.
This real-time statistical data measured in the direction of the satellite provides an estimate of the phase front distortion experienced at the same time by the NOEMA interferometer.

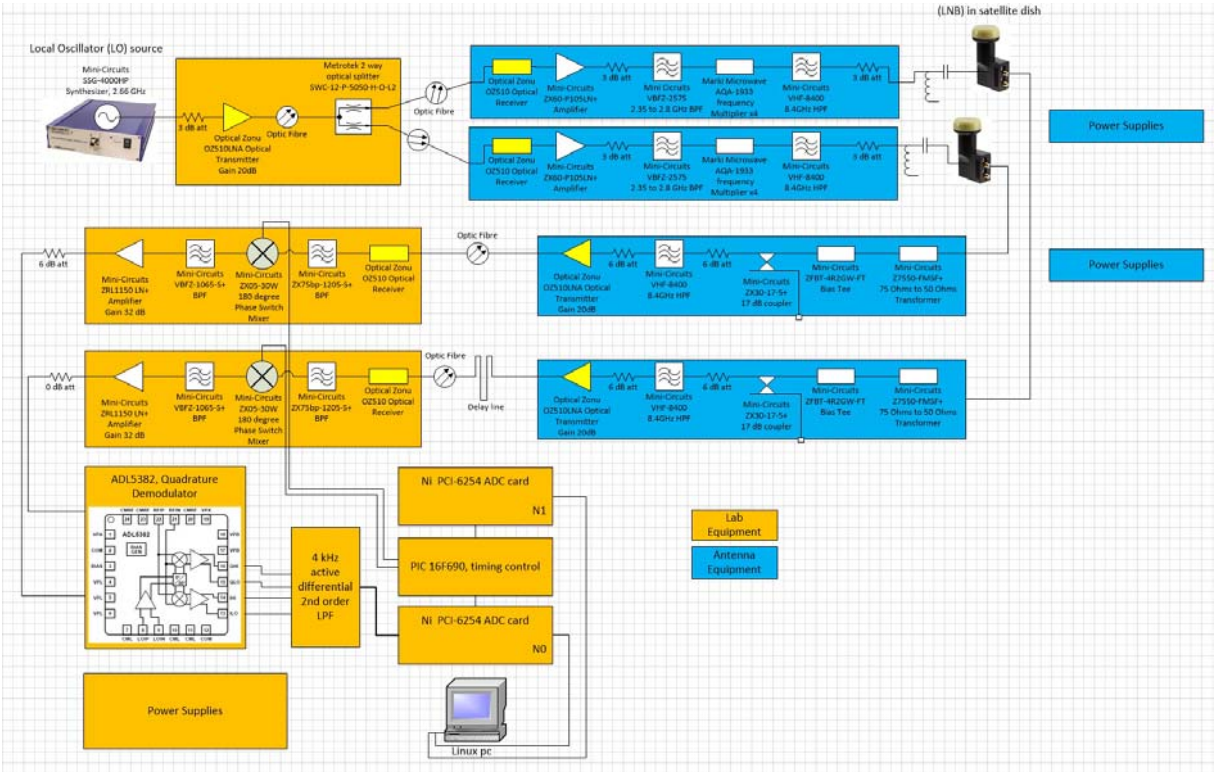

Figure 3: Dual Antennas Phase Monitoring System Schematic. Equipment highlighted in orange are located in the laboratory racks, while blue ones are situated in the antenna racks.

3 Phase Monitoring System Implementation

3.1 Improvements

During the development phase at the IRAM headquarters, located in St Martin d'Hères on the university campus, some optimizations were implemented in order to achieve the best possible results. The list is detailed below:

- Addition of strengthening aluminium tubes between parabola and LNB to ensure good mechanical stability
- Meticulous analysis and suppression of EMC related noise by addition of dedicated filtering on the DC lines, separation of IQ demodulation board and IF switch boards, use of low noise power supplies
- Use of a phase shifter to calibrate the IQ gain and offset errors
- Use of Mini-Circuits synthesizer for LO frequency generation
- First use of Technomate LNB, detailed study of effect of LO power fluctuation
- LO injection into LNB DRO amplifier input
- Use of Marki Microwave x4 frequency multiplier in LO circuit to reduce LO part count
- Use of Optical Zonu LNA transmitter to reduce IF and LO part count (fewer amps)
- Detailed study of phase shifter balance
- Implementation in the antenna racks of lightning protections

3.2 Rack Setup

Every box shown on Figure 3 materialises a mechanical enclosure that takes place either in a rack of electronic that is located in the laboratory or in a rack that is attached to the antenna pole. The Figure 4 shows the antennas on the roof of IRAM headquarters and laboratory rack of electronics.

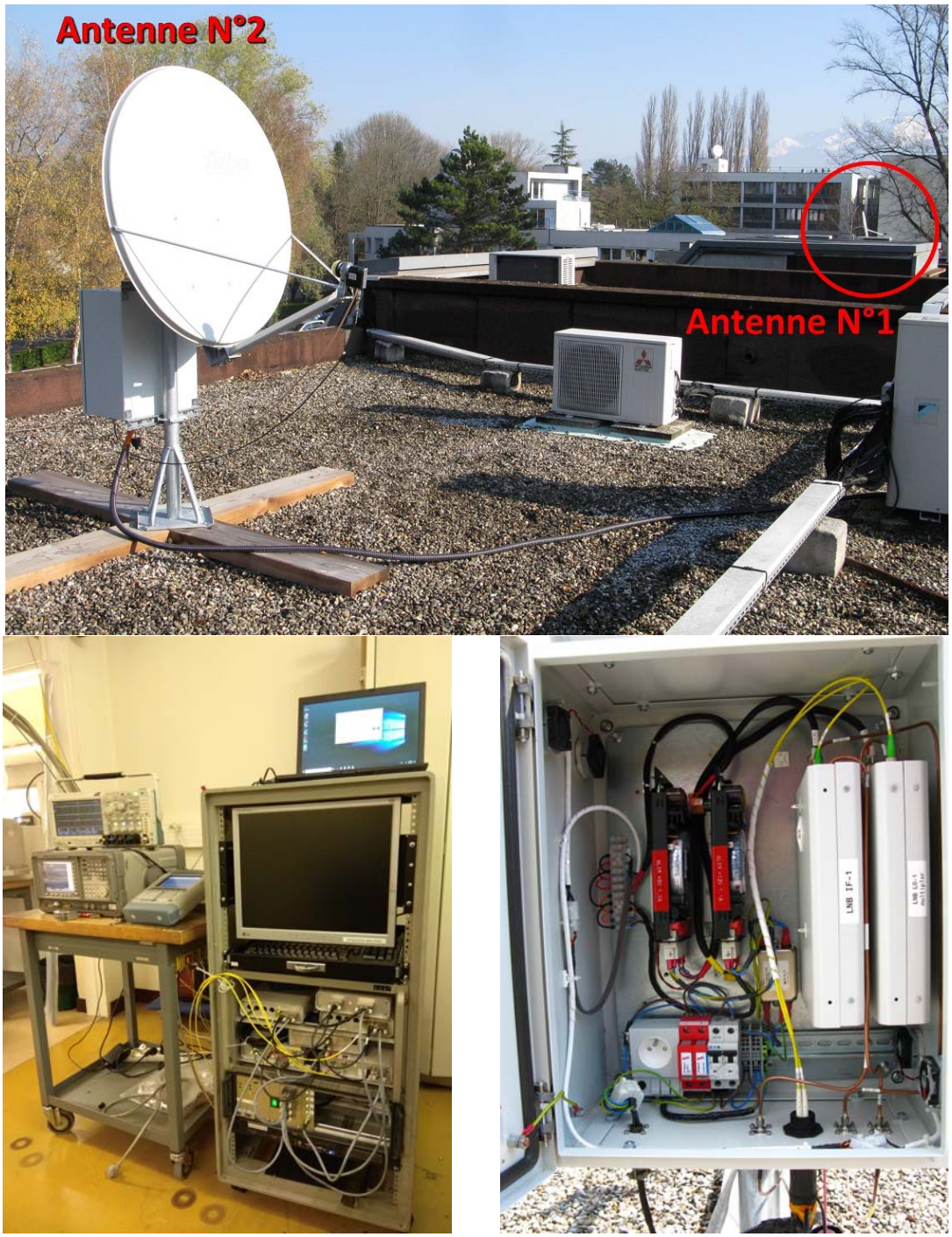

Figure 4: Top: Antennas on the IRAM headquarters roof in Grenoble. Bottom left) Indoor rack of electronics and control pc, Bottom right) Outdoor rack of electronics.

3.3 Data collection

After the initial tests carried out at the IRAM headquarters, where we were facing electromagnetic pollution and environmental limitation, the system was moved to Plateau de Bure in mid-October to make onsite observations before the coming of the winter: All-year operation of such a system requires a protective infrastructure (radomes or similar shielding) due to electronics vulnerability to the meteorological conditions of the site.

The goal of this experiment was to compare the measured satellite phase with the observed NOEMA interferometer phases. The two-element satellite interferometer operating at 11.85 GHz was installed on the Eastern NOEMA track, with the antennas pointing towards the south, with no NOEMA antennas in front

(see Figure 5). The system spanned a baseline of 40 meters close to the E18 and E23 pads, and pointed to the geostationary ASTRA 3B satellite under an azimuth of -24.3° (with 0°=South, and negative numbers East) and an elevation of 35.7°.

Figure 5: One Atmospheric Phase Monitor Antenna on E18 pad, next to a 15 meters NOEMA Array antenna.

3.4 Data Analysis

The phase monitor system was installed and running on the plateau de Bure for a limited amount of time, before harsh winter weather condition occur and between two NOEMA interferometer configuration changes. During that period, two sets of data were collected, separated by a gap on the graph.

The measured fringes of the phase monitoring interferometer contain the traces of the satellite movement around its equilibrium point. A succession of second-order polynomial was fitted over several intervals, until the end of the recording where a final fit was made. The overlapping polynomials were then combined with a Gaussian weighting that dropped to 5% at the edges of each interval.

The result of this operation can be seen in Figure 6 left. For further analysis and comparison with NOEMA observations, the phase noise was converted from degrees phase to optical path microns. Phase noise was then studied over two timescales: 135 seconds corresponding to the duration of one NOEMA phase calibration, and 1 second for a consistency check of the phase information. Tropospheric water vapour being distributed in bubbles with a power-law size distribution; phase noise caused by turbulent water vapour is expected to rise according to a power law and level off at the outer edge of the turbulence, or at the length of the maximum baseline. From this behaviour one would expect a higher phase noise at 135 seconds than over a timescale of one second. The plot in Figure 6 right shows that the expected behaviour for tropospheric water vapour phase noise is fulfilled until about midnight UT on October 27 (passing from October 26th to 27th) but that there is a significant short-term phase noise contribution later. This noise must have a different reason than atmospheric water vapour, either instrumental (wind-induced vibrations) or due to external reasons like ionospheric activity.

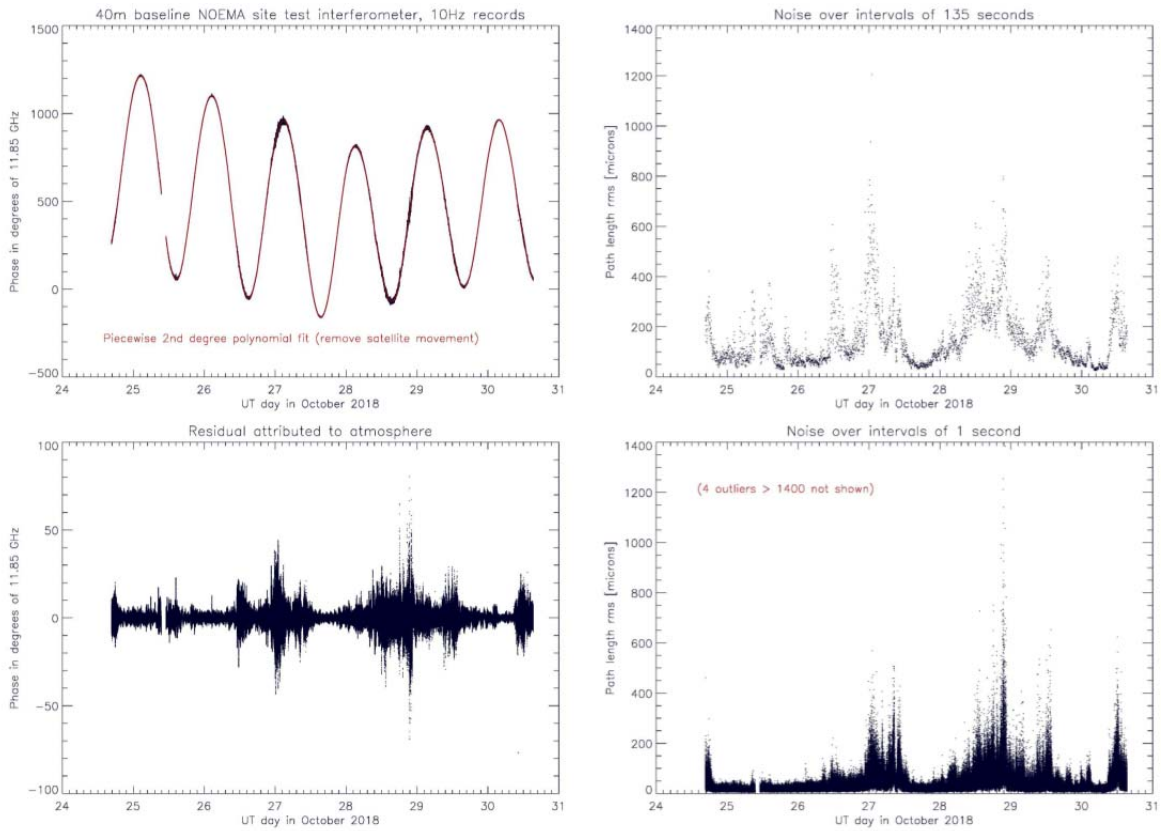

Figure 6: Left) Measured Satellite Interferometer Phase, sampling 10 Hz, Right) Phase Noise over intervals of 135 seconds and 1 second, in microns.

For comparison with NOEMA observations, archival interferometer data were retrieved and the calibrator phase noise for each 135 second phase calibrator observation calculated. The degrees phase were then converted to microns of optical path and sorted by baseline length. A linear fit in the log-log diagram of baseline length vs. noise was used to derive the optical path variations at 40 meters, i.e. the baseline length of the site test interferometer. The resulting superposition of satellite phase and observed phases is shown in Figure 7, together with the meteorological records of the NOEMA weather station. To confirm the correct time alignment between the data sets, the weather records of the NOEMA archived files are superimposed in green on the graphs.

Finally, observing conditions and antenna pointing information are compiled in Figure 8. It shows that the site test interferometer gives a reasonable optical path noise estimate under a variety of observing frequencies and observing directions, i.e. the fact that the satellite dishes always point to the same direction was not a fundamental problem in the monitoring of the all-sky observing conditions, at least not under the conditions during this test.

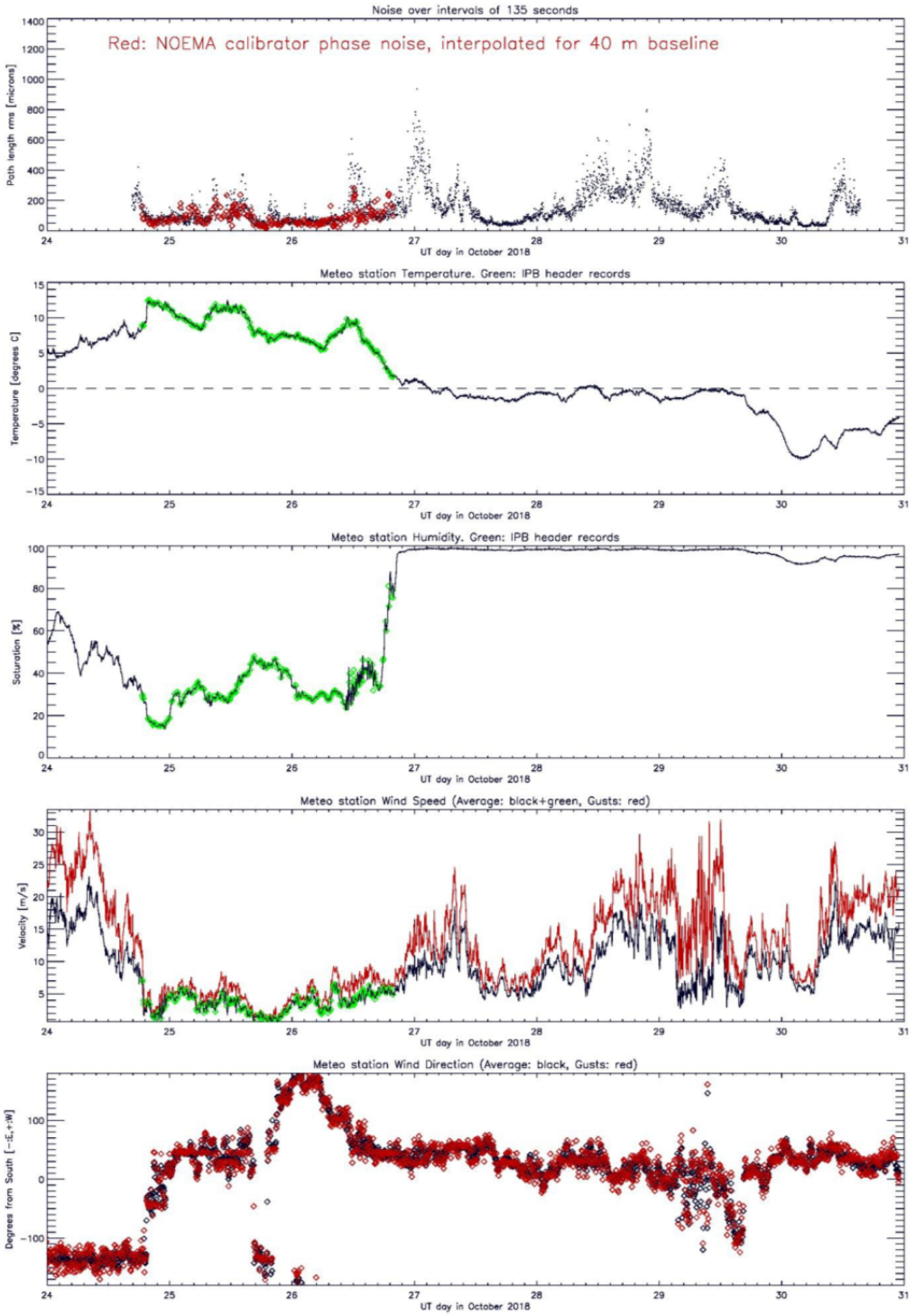

Figure 7: Phase Noise of Test Interferometer and NOEMA, with weather records.

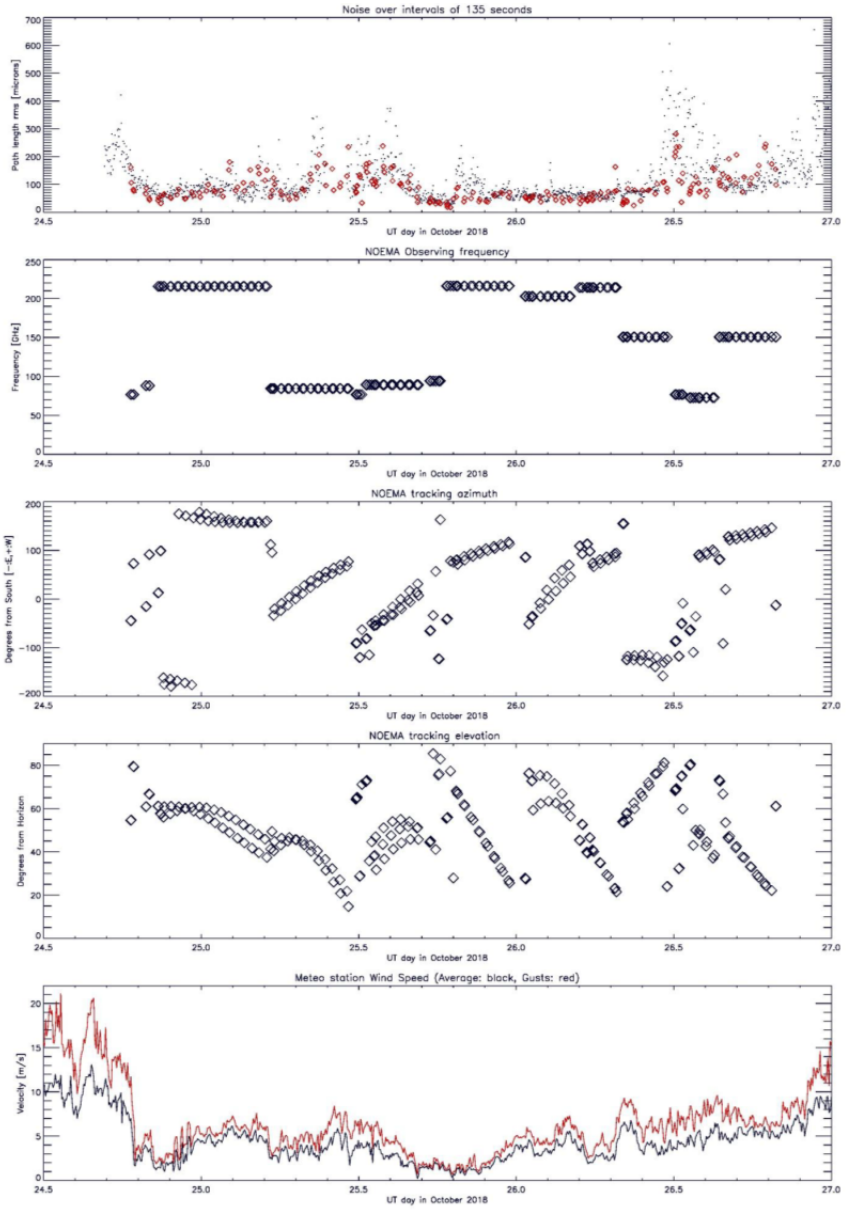

Figure 8: Phase Noise and NOEMA Tuning Frequency, Pointing Information and Wind.

4 Conclusion

This paper has described the phase monitoring system work that has been ongoing for the past two years at IRAM. It described in details the hardware that has been used, together with the first encouraging results that were obtained on the plateau de Bure. A new campaign of data collection will occur in the coming months. In order to make sure that the system is not affected by the environmental conditions, we plan, this time, to protect the antennas in some kind of shelter like radome or else.

Références bibliographiques

[1] Robert S. Kimberk & All “A Multi-Baseline 12 GHz Atmospheric Phase Interferometer with One Micron Path Length Sensitivity”, May. 2012.